PAPER A

INTEGRATED CROSSWELL IMAGING: REFLECTION TOMOGRAPHY– SYNTHETIC EXAMPLES

Mark A. Van Schaack

ABSTRACT

Last year I introduced a proposal to integrate the processing of crosswell reflection imaging and traveltime tomography. I have modified this scheme to allow an interpretation of the reflection image to be used to guide the picking of reflection traveltimes. This requires an ability to map reflection data using the 2-D traveltime tomogram and to inverse map, or forward model, the interpreted reflections.

I am currently working on programming the various processors required in the integrated iterative inversion. A program allowing the simultaneous inversion of reflection and direct arrival traveltime picks is now complete. Traveltime inversions run on synthetic data show that including reflections in the traveltime inversion improves the imaging ability at the top and bottom of the surveyed zone where ray coverage is typically poor for direct arrivals. Also, reflection tomography improves the vertical resolution midway, between the wells. This improvement in resolution is required to reduce the "dog bone" and "football" artifacts which occur as a result of bowed interfaces.

INTRODUCTION

An approach to integrating crosswell reflection imaging and traveltime tomography was presented by Van Schaack and Lazaratos (1993). As observed by Lazaratos (1993), inaccuracies in the velocity model used in the XSP-CDP mapping technique result in lateral and vertical mispositioning of reflection events. These mispositioning errors cause destructive interference when stacked and result in a loss of resolution in the reflection image. An inversion was proposed which perturbs the velocity model to minimize these errors. Although this inversion is similar in philosophy to surface seismic velocity analysis it is better described as crosswell reflection traveltime tomography (CRTT). It utilizes both direct and reflected arrival traveltimes in a single inversion for the velocity field.

There are a number of different ways in which CRTT can be parameterized and solved. It would be preferable to solve for "everything", e.g., a finely-gridded, fully 3-dimensional anisotropic velocity distribution including the location and orientation of arbitrarily defined reflectors. Unfortunately, even a simple 2-dimensional isotropic velocity inversion may end up being underdetermined if care is not taken in defining the gridding. To optimize a solution, the parameterization should be made to reduce the number of variables wherever possible. An example of this in CRTT is a parameterization developed by Michelena (personal comm.) which solves for the location and dip of linear interfaces and the velocity of homogeneous isotropic layers. In a geology where layers can be accurately described as constant velocity, this parameterization might be ideal.

In this paper I review a philosophy of integrated reflection and tomographic inversion. This philosophy determines the parameterization of the reflection traveltime inversion. A number of synthetic examples are presented to illustrate the potential of including reflections in crosswell traveltime tomography. Finally, I discuss the next steps required to apply this technique to real data.

PHILOSOPHY OF THE INTEGRATED CROSSWELL INVERSION

Background

A large number of the published crosswell studies have been of areas where the geologic structure is predominantly flat or mildly dipping (homocline). Examples of this are: Amoco/Conoco's North Cowden study, West Texas (Lines et al., 1993), Stanford/Chevron's McElroy study, West Texas (Harris et al., 1992), Exxon's Friendswood test site, Texas (Chen et al., 1990) and BP's Devine test site, West Texas (Harris, 1988). Areas with simple geologic structure are ideal for CRTT since structural interpretation of the reflection image is relatively straightforward and easily checked against the well log interpretation. If reflectors can be found, and their orientations determined manually, the reflection tomography problem is much simpler.

If the structure is simple, what is the benefit of crosswell imaging? There are several potential uses of crosswell imaging in simple structures. One application is reservoir characterization. Even when the basic structure of the geology is simple, stratigraphic variations within layers can exist. These stratigraphic variations may result from primary depositional processes, or from secondary infilling or enlargement of the pore space. Secondary processes are occasionally the direct result of oil production and injection programs. These variations may be measured seismically as small velocity perturbations. A

second application is monitoring. The injection of fluids in a reservoir may be monitored directly with crosswell imaging if the injected fluid results in a seismic velocity change.

Both of the above applications, reservoir characterization and monitoring, benefit from the highest resolution, most accurate information available. One of the advantages of integrating reflection imaging and traveltime tomography is that resolution and accuracy are added to both. In this paper I will describe an approach to integrated inversion using CRTT. This approach is designed to work optimally when the basic geologic structure is simple and the crosswell reflection images can be interpreted in a straightforward manner.

Simple structures

The definition of simple structure that I have used in the design of the integrated inversion is subject to several conditions:

1) Reflectors must be interpretable from the crosswell reflection image

2) Each interpreted reflector must intersect both wells

3) Each interpreted reflector must expressible as a function of horizontal, interwell offset

These conditions are required to define the position of each reflector in terms of a simple equation. For the i'th reflector, the depth of that reflector is defined as a function of offset,

$$z_i = f_i(x) \tag{1}$$

In this equation, z_i is the reflector depth, and x is the horizontal offset. The $f_i(x)$ is a function describing the i'th reflector which is determined from the interpreted reflection image.

THE INTEGRATED INVERSION

Data preparation

Figure 1 is a schematic of the integrated crosswell imaging procedure. Prior to the iterative imaging process the crosswell data are processed in a standard fashion. First, direct arrival traveltimes are picked from the raw waveforms. The next step is wavefield separation and reflector enhancement. Typically traveltime picks are used to design filters to perform this processing (Rector, 1994). The results of these steps, the direct arrival traveltimes and the processed wavefield, are passed to the iterative integrated inversion.

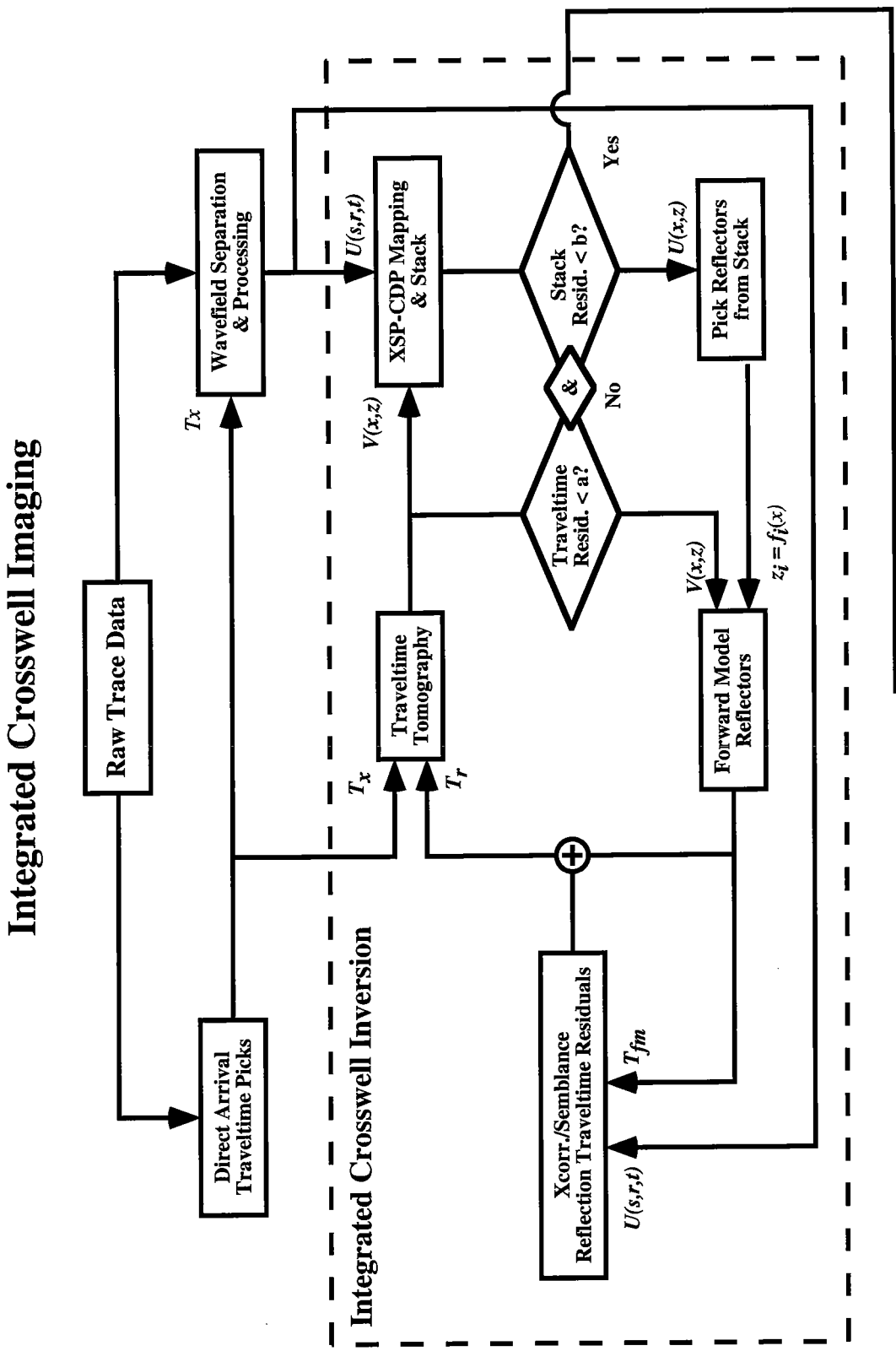

Figure 1: This schematic outlines a processing technique which integrates crosswell traveltime and reflection data in a single inversion. This technique is iterative and requires interpretation of the reflection image after each mapping to define reflector locations and orientations.

Iterative Inversion: Step 1 – Direct Arrival Tomography and Reflection Imaging

The first step in the iterative inversion is direct arrival traveltime tomography. The traveltime inversion is run in a standard fashion to calculate a 2-D velocity model. The result of the velocity inversion, a velocity map, $v(x,z)$, is passed to the mapping routine. The mapping and stacking process is performed in a similar manner to that described by Lazaratos (1993). There are two differences to Lazaratos' technique. First, a fully 2-D mapping algorithm is used to accommodate the 2-D traveltime tomogram. Second, the "residual statics" step, used to line up reflection events prior to stacking, is not required.

The purpose of residual statics processing is to align reflections prior to stacking to ensure an optimal stack. The use of the residual statics technique was originally justified by several reasons (Lazaratos, 1993). The XSP-CDP mapping algorithm used by Lazaratos was designed to use only a 1-dimensional velocity models. Also, corrections were not made for well deviations. The McElroy data processed using this technique were collected in a setting where the geology was primarily layer-cake and well deviations were mild. The validity of the 1-D and straight well assumptions was supported by the observation that the mispositioning of the reflection events, prior to stacking, was also rather mild. Nevertheless, Lazaratos found that additional resolution could be obtained in the reflection image by "forcing" the reflectors to align. This technique is similar to "non-surface consistent statics", which is used occasionally in surface seismic data processing. Since I intend to use a 2-D mapping algorithm, which will also correct for well deviations, the residual statics technique should not be necessary.

Iterative Inversion: Step 2 – Convergence test

These decision boxes, seen in Figure 1, following the traveltime tomography and reflection imaging, test the images for convergence. Acceptable limits for convergence are primarily subjective and the number of iterations performed may be determined, in reality, by available computer and human resources. If the convergence criteria are met, the velocity tomogram and reflection image are judged acceptable and the processing is finished.

Iterative Inversion: Step 3 – Reflector picking from stacked reflection image

In this step the two reflection images, upgoing and downgoing, are interpreted. Although nothing prohibits the use complex dipping structures the algorithm has been designed to use reflectors defined as single-valued functions of offset. This is done to

simplify several steps: the definition of the reflector, inverse mapping (not yet discussed), and raytracing. Equation (1) provides the mathematical description of the reflection events. Any phase can be used to define the reflector: peaks, troughs, zero crossings, or an intermediate phase. The important point is that this same phase must be used to identify the reflections in the space-time domain.

The reflection events are picked separately from the upgoing and downgoing sections. In practice, the downgoing section is typically the best at the top of the surveyed zone and the upgoing section is the best at the bottom. Past experience suggests that the number of events that are imaged by both up and downgoing events is not that large. The small number of these twice imaged reflections, plus the difficulty of ensuring that the events picked actually are the same reflection, suggests that the inversion is best parameterized without them.

Iterative Inversion: Step 4 – Inverse mapping reflection events

The traveltime tomogram and picked reflection events are next input to the inverse mapping routine. Inverse mapping, as it is used here, is essentially forward modeling. For a given source-receiver-reflector combination, and an assumed velocity model (the traveltime tomogram), a traveltime is calculated. This time is calculated using an energetic-arrival finite-differences eikonal solver (Mo, 1994). This solver is used to calculate two traveltime maps using the traveltime tomogram as the velocity model. One map is calculated using the source's location and another map is calculated using the receiver's location. These two maps are then added together. The resulting combined traveltime map defines the traveltime from every point on the image to the source and receiver. Described another way, the traveltime from the source, to a point, to the receiver, is stored at the location of that point.

For a particular reflector, the reflection traveltime can be found on the combined traveltime map as the minimum time on that reflector's trajectory. This approach is an application of Fermat's principle. Forward modeled traveltimes for each source-receiver-reflector combination are calculated and stored for both upgoing and downgoing images.

Iterative Inversion: Step 5 – Reflection traveltime residuals

Step 4, inverse mapping/forward modeling, calculates the traveltimes of reflected events using with the traveltime tomogram as the velocity model. If the traveltime tomogram is "correct", in other words, accurately reflects the true velocities of the medium, several observations can be made:

1) The traveltime residual of the tomographic inversion will be zero (or a minimum)

2) There will be no misalignments of reflection events in the pre-stack, mapped reflection data

3) The reflection traveltimes calculated in step 4, forward modeling, will equal the observed reflection traveltimes

Since step 5 is reached by failing the convergence test, step 2, observations 1 and 2 are not true. The failure of the convergence test also ensures that observation 3 will be untrue.

In step 5 the residual error, r, is calculated. The residual error is the difference between the forward-modeled reflection traveltimes and the observed reflection traveltimes. This can be expressed as

$$r = t_{obs} - t_{calc} \tag{2}$$

The observed traveltime used in the tomographic inversion, can be calculated by adding the residual to the calculated traveltime. This indirect approach to obtaining the true reflection traveltimes is necessitated by the fact that reflections are normally very difficult to see even in the processed data. By calculating the reflection traveltimes as a perturbation of a predicted set of times, the search window can be focused, minimizing errors.

There are several approaches to obtaining the reflection traveltime residuals. The most direct approach, although very labor intensive, is to manually correct the traveltimes in the space-time domain. This produces the observed traveltimes directly. By perturbing the forward-modeled times the residual is added in one step. The disadvantage of this technique is that it is so labor intensive that it would be difficult to process a large number of reflectors in a reasonable time. The advantage is that this technique allows the human operator to interpret and reject noise that might overwhelm other techniques.

A more automated approach is to use a semblance, correlation, or maximum coherency technique. Each of these has its own advantages and disadvantages which are currently under study. The primary motivation for research in this area is that a robust automated traveltime picker will allow a large number of reflectors to be processed.

Iterative Inversion: Step 6 – Completing the iteration with CRTT

The final step of the combined iterative inversion is to use both reflection and direct arrival traveltimes in a single tomographic inversion. Mathematically, the combined inversion is identical to the inversion using only direct arrivals. For each source-receiver-reflector combination where a traveltime is obtained, a raypath can be computed and a

traveltime calculated. The difference between observed and calculated traveltimes is then backprojected along the raypath. This is done for all reflection and direct arrival traveltimes and iterated until a convergence criteria is met. The output velocity model is then passed along to the mapping routine for processing and the entire process is repeated again.

CROSSWELL REFLECTION TOMOGRAPHY — SYNTHETIC EXAMPLES

Introduction

There are several algorithms to build in order to implement the integrated crosswell inversion. In this section I show the results of two synthetic crosswell reflection traveltime inversions. The algorithm used in these crosswell inversions uses a SIRT inversion scheme parameterized with orthogonal pixels describing a 2-D velocity image. Raytracing is performed with an initial value ray tracer described by Harris (1992).

These inversions simulate the final iteration of the integrated inversion process. In the final iteration, reflector geometries are known and the reflection traveltimes are considered accurate. With accurate direct arrival and reflection traveltimes, the traveltime inversion is run to convergence to obtain the optimum velocity image. The results of these inversions show the potential of a combined reflection and direct traveltime inversion.

Simulation 1 — A simple 3-layer model

Figure 2 shows the simple 3-layered model used in the first simulation. The data set for this model consists of 101 source by 101 receiver locations. Reflection traveltimes are modeled for 4 reflectors: one at the top of the surveyed zone, one at 200 ft, one at 300 ft, and one at 500 ft, the bottom of the surveyed zone. Both upgoing and downgoing reflection traveltimes are calculated for each reflector.

Examples of the traveltime picks used in the inversion are shown in Figure 3. The direct arrival picks are displayed (Figure 3a) with the receiver elevation on the horizontal axis and source elevation on the vertical axis. The reflection traveltime picks for the 200 ft reflector are shown in Figure 3b. The same display is used for these picks. Note that a large part of the receiver pick map is zero valued. These null values occur at source and receiver positions that straddle the reflector. One of these pick maps is required for each reflector used in the traveltime inversion.

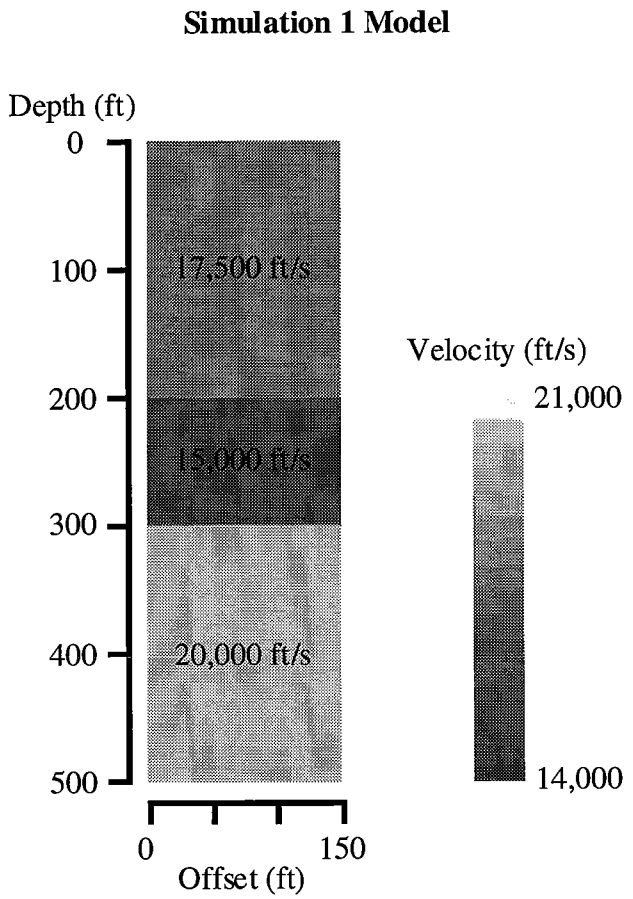

Figure 2: A simple 3-layered model used to generate traveltime data for a combined direct arrival and reflected arrival traveltime inversion. The shooting geometry is 101 sources by 101 receivers evenly spaced every 5 ft down the sides of the model.

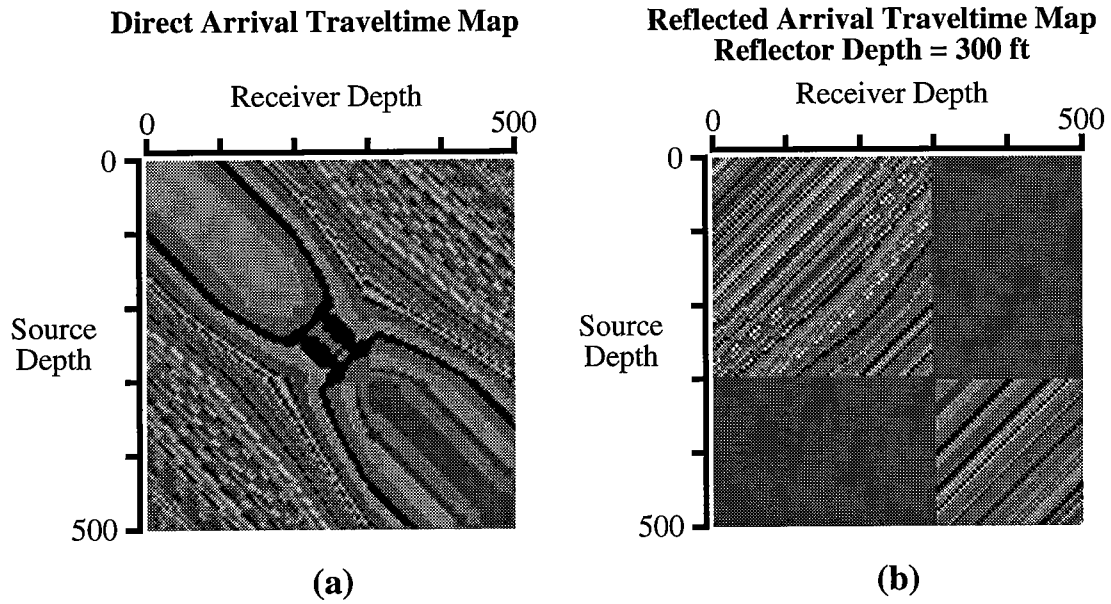

Figure 3: Direct arrival (a) and reflected arrival (b) traveltime maps. These images are displayed using a "random" colortable to accentuate the isochron contours of the pick images. Figure 3b is an example of reflected arrival traveltime picks for a horizontal reflector at 300 ft. The homogeneous gray areas of the map are null picks. This occurs when the source and receiver locations straddle the reflector and no reflection is possible. Both up and downgoing reflection picks are present on this image.

The results of the traveltime inversions are shown in Figure 4. Figure 4a is the model used to create the traveltime data. Figure 4b is the final image of a traveltime inversion using only direct arrivals . Figure 4c is the final image of the traveltime inversion using both direct and reflected arrivals. Both of these inversion were run in an identical manner: 10 iterations with 4 backprojections for each inversion.

The most obvious improvements seen in the reflection traveltime tomogram can be found in the vicinity of the interfaces located at 200 and 300 ft. The bowing in the interfaces seen in Figure 4b, a common artifact in crosswell traveltime inversions, is virtually eliminated by including the reflection traveltimes. Lateral variations in the top and bottom layers in Figure 4b are also absent in the reflection traveltime tomogram.

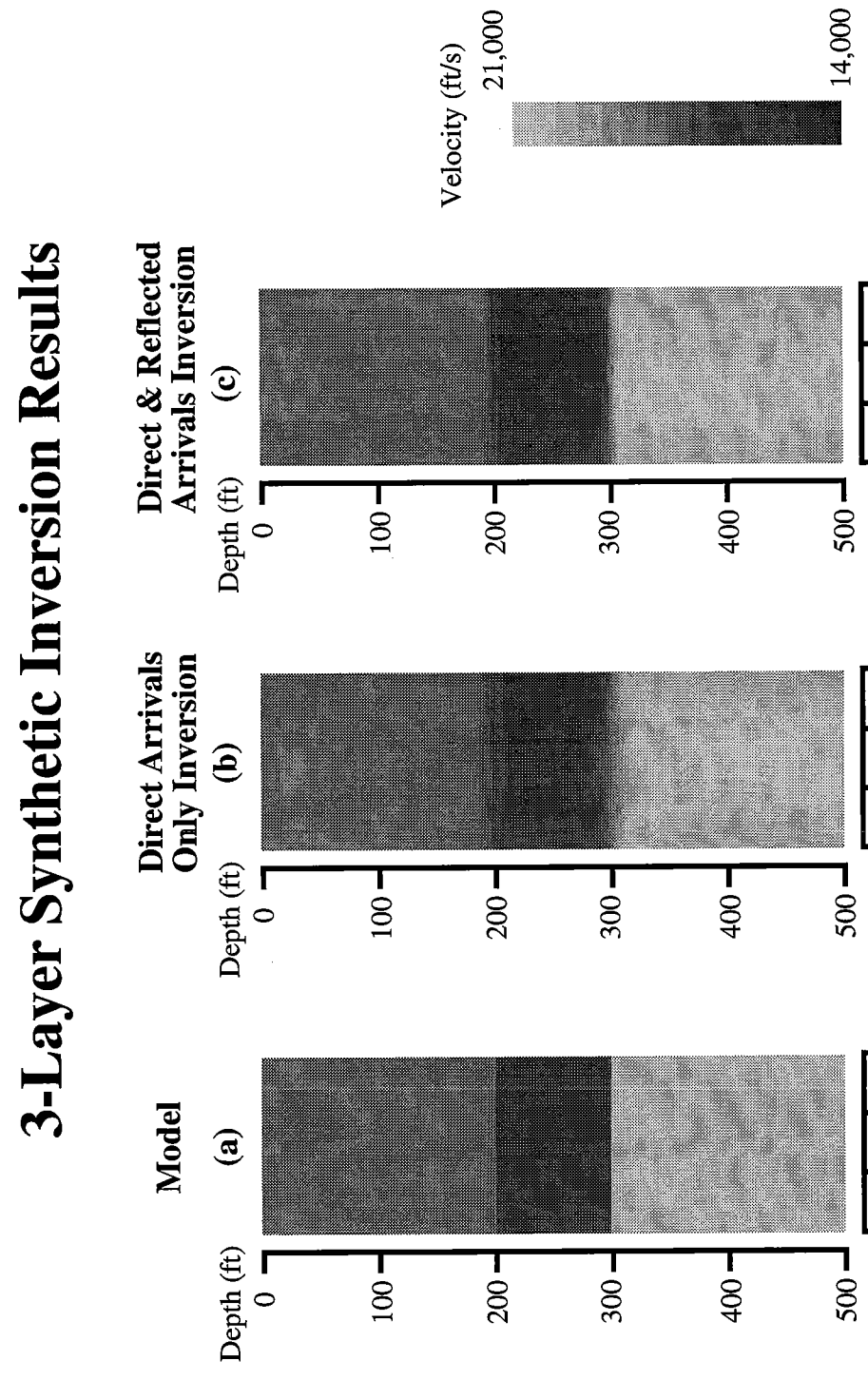

Figure 4: The above results provide a comparison of an inversion calculated with both direct and reflected traveltime arrivals (c), and an inversion run using only direct arrivals (b). Both inversions were run identically: 10 iterations, 4 backprojections each iteration.

Simulation 2 — A 7-layer model

Figure 5a shows the model used in the second simulation. This model includes 7 layers and reflection traveltime picks were used for all 8 interfaces, which includes the top and bottom of the model. Traveltime inversions were run using only direct arrival picks and combined direct arrival and reflected arrival picks. Again, the inversions were run identically. In this test, 10 iterations were calculated with 20 backprojections for each iteration. The source and receiver geometries are identical to the first simulation: 101 source by 101 receiver locations spaced evenly every 5 ft.

The results of simulation 2 are shown in Figures 5b and 5c. The improvements offered by the combined inversion are essentially the same as seen in simulation 1. The artifacts in Figure 5b are comparatively larger than those seen in Figure 4b. This is a result of the interfaces near the top and bottom edges of the model where ray coverage and resolution are poor.

CONCLUSIONS

Integrated iterative inversion of crosswell reflection and traveltime data can potentially lead to improvements in the resolution obtainable in crosswell imaging. In this paper I outline a scheme by which these data can be simultaneously processed. Nearly all of the programs required to accomplish this processing are in place. The next step will be to write a general 2-D mapping program which corrects for well deviations and to automate reflection traveltime picking so that large numbers of reflections can be processed.

The combined reflection and traveltime inversion offers improvements in the resolution of interfaces near the middle of the surveyed region. Also, improvements in resolution are seen at the top and bottoms of the surveyed zone where transmission traveltime tomography fails due to poor ray coverage.

ACKNOWLEDGMENTS

I would like to thank Bob Langan, Le-Wei Mo, and Spyros Lazaratos for their useful discussions on the topic of reflection imaging and traveltime tomography. I would also like to thank the corporate sponsors of the Stanford Tomography Project for their continued support.

7-Layer Synthetic Inversion Results

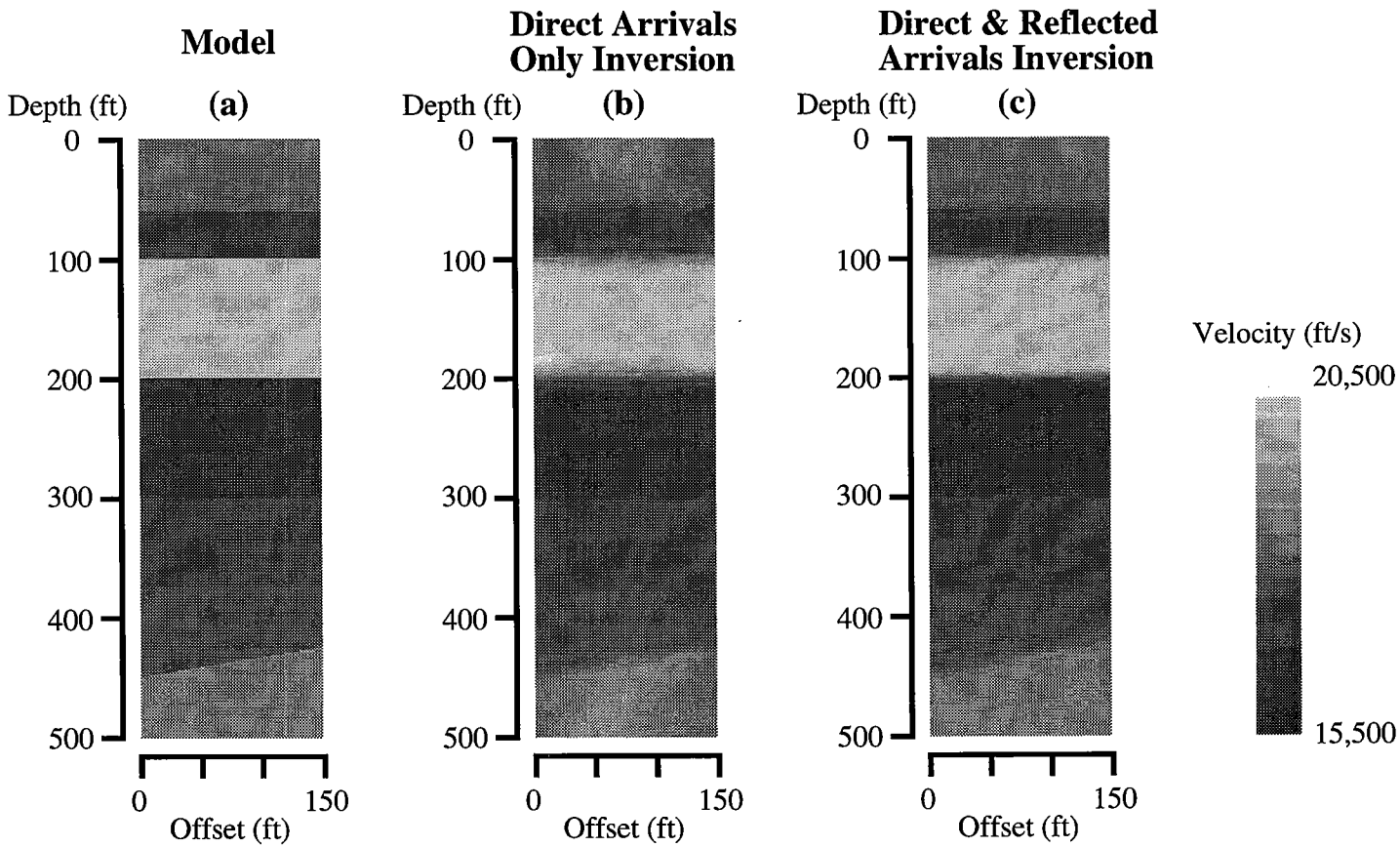

Figure 4: The above results for the more complex 7-layer model provide another comparison of an inversion calculated with both direct and reflected traveltime arrivals (c), and an inversion run using only direct arrivals (b). Both inversions were run identically: 10 iterations, 20 backprojections each iteration.

References

Chen, S.T., Zimmerman, L.J. and Tugnait, J.K., 1990, Subsurface imaging using reversed vertical seismic profiling and crosshole tomographic methods: Geophysics, **55**, 1478-1487.

Harris, J.M., 1992, Initial value raytracing in smoothly varying heterogeneous media: STP-**3**, paper I.

Harris, J.M., Nolen-Hoeksema, R., Rector, J.W., Van Schaack, M.A., and Lazaratos, S.K., 1992, High resolution cross-well imaging of a West Texas carbonate reservoir: Part 1. Data acquisition and project overview: 62nd Ann. Internat'l Mtg., Soc. Expl. Geophys., Expanded Abstracts, 35-39.

Harris, J.M., 1988, Cross-well seismic measurements in sedimentary rocks: 58th Ann. Internat'l Mtg., Soc. Expl. Geophys., Expanded Abstracts, 147-150.

Lazaratos, S.K., 1993, Cross-well reflection imaging: Ph.D. thesis, Stanford University.

Lines, L., Tan, H., Treitel, S., Beck, J., Chambers, R., Eager, J., Savage, C., Queen, J., Rizer, W., Buller, P., Cox, D., Ballard, J., Kokkoros, G., Sinton, J., Guerendel, P., Track, A., Harris, J., Lazaratos, S., Van Schaack, M., 1993, Integrated reservoir characterization: Beyond Tomography: 63rd Ann. Internat'l Mtg., Soc. Expl. Geophys., Expanded Abstracts, 298-303.

Mo., L.W., 1994, Calculation of direct arrival traveltimes by the eikonal equation: STP-**5**, paper K.

Rector, J.W., Harris, J.M., Lazaratos, S.K., and Van Schaack, M.A., 1994, Multidomain analysis and wavefield separation of cross-well seismic data: Geophysics, **59**, 27-35.

Van Schaack, M.A. and Lazaratos, S.K., 1993, An approach to interval velocity analysis for crosswell reflection imaging using reflection traveltimes: STP-**4**, paper F.